Colloids and Surfaces B: Biointerfaces 186 (2020) 110682

Contents lists available at ScienceDirect

Colloids and Surfaces B: Biointerfaces

journal homepage: www.elsevier.com/locate/colsurfb

Micro-patterned SU-8 cantilever integrated with metal electrode for enhanced electromechanical stimulation of cardiac cells

Nomin-Erdene Oyunbaatar[a], Arunkumar Shanmugasundaram[a], Yun-Jin Jeong[a], Bong-Kee Lee[a], Eung-Sam Kim[b], Dong-Weon Lee[a,c,*]

[a] School of Mechanical Engineering, Chonnam National University, Gwangju-61186, Republic of Korea
[b] Department of Biological Sciences, Chonnam National University, Gwangju, 61186, Republic of Korea
[c] Center for Next-generation Sensor Research and Development, Chonnam National University, Gwangju, 61186, Republic of Korea

ARTICLE INFO

Keywords:
Cardiomyocytes
Cantilever
Stimulation
Contraction force
Drug toxicity screening

ABSTRACT

Over the past few years, cardiac tissue engineering has undergone tremendous progress. Various *in vitro* methods have been developed to improve the accuracy in the result of drug-induced cardiac toxicity screening. Herein, we propose a novel SU-8 cantilever integrated with an electromechanical-stimulator to enhance the maturation of cultured cardiac cells. The simultaneous electromechanical stimulation significantly enhances the contraction force of the cardiomyocytes, thereby increasing cantilever displacement. Fluorescence microscopy analysis was performed to confirm the improved maturation of the cardiomyocytes. After the initial experiments, the contractile behaviors of the cultured cardiomyocytes were investigated by measuring the mechanical deformation of the SU-8 cantilever. Finally, the proposed electromechanical-stimulator-integrated SU-8 cantilever was used to evaluate the adverse effects of different cardiac vascular drugs, *i.e.*, verapamil, lidocaine, and isoproterenol, on the cultured cardiomyocytes. The physiology of the cardiac-drug-treated cardiomyocytes was examined with and without electrical stimulation of the cardiomyocytes. The experimental results indicate that the proposed cantilever platform can be used as a predictive assay system for preliminary cardiac drug toxicity screening applications.

1. Introduction

Although medical diagnosis, treatments, and prevention have undergone substantial development, cardiovascular diseases remain a significant concern to human health [1]. Cardiovascular diseases are the leading global cause of death, accounting for 17.3 million deaths per year. This number is expected to increase to > 23.6 million by 2030. According to a recent study performed by Benjamin et al., 106000 Americans die every year as a consequence of taking prescribed cardiovascular medications, and nearly five times the number of people killed by the adverse effects of cardiovascular drugs [2]. The side effects of such drugs are among the several factors for the high rate of heart failures [3]. Thus, cardiac diseases due to the adverse effects of cardiac drugs is a significant health risk; therefore, addressing it should be considered a global health priority. At present, a patch-clamp assay is widely used to recognize the side effects of cardiovascular drugs at an early stage of drug discovery [4]. Numerous electrophysiological methods have been developed to analyze drug-induced cardiac toxicity effects [5,6]. For instance, the microelectrode-array-integrated biosensing platforms have been developed for measuring the electrophysiological characteristics, such as field potential and impedance, of drug-treated cardiomyocytes [7]. However, the development of new methods is still required for ensuring the reliability of the drug-induced cardiac screening platform.

Recently, several techniques, including mechanical/electrical stimuli, have been developed to support the results of electrophysiological methods [8]. These techniques use the principle of mechano-transduction to investigate the electrophysiological characteristics of the cardiomyocytes. Another type of stimulus is the utilization of the geometry of substrates. This stimulus allows the cells to take advantage of the environment during growth [9]. Such techniques typically utilize two-dimensional or three-dimensional (3D) cell culturing platforms with micro- or nanosized groove patterns. The surface-patterned sensing platform efficiently stimulates cell–cell proximity, enhances cell self-assembly and improves the overall tissue function [10]. For instance, a microgroove (μgroove)-patterned cantilever is effective for

* Corresponding author at: MEMS & Nanotechnology Lab, School of Mechanical Engineering, Chonnam National University, 77 Yongbong-ro, Buk-gu, Gwangju 500-757, Republic of Korea.
E-mail address: mems@jnu.ac.kr (D.-W. Lee).

https://doi.org/10.1016/j.colsurfb.2019.110682
Received 10 May 2019; Received in revised form 29 October 2019; Accepted 27 November 2019
Available online 28 November 2019

improving cell maturation and investigating the contractile behaviors of drug-treated cardiomyocytes [11]. Among the various proposed polymer-based cantilevers, the SU-8 material has received considerable attention because of its biocompatibility and excellent capability for mass production. In addition, SU-8 exhibits the desirable cell adhesion property and efficiently transmits the resultant contractile force. Thus, the SU-8 cantilever exhibits large bending displacement and can identify small changes in the contractility of the cardiomyocytes [12]. Recently, electrical-stimulation-based cell culture platforms have been developed to improve the maturation of the cultured cardiomyocytes. The applied electric field triggers an action potential related to the ion flux through the cell membranes [13]. In recent studies, the benefits of electrical stimulation were effectively utilized [14], and arrhythmia [15], mechanoelectrical feedback [16], and contraction and relaxation of cardiomyocytes were successfully detected. All the proposed methods have advantages and limitations in terms of the precision, physiological significance, and scalability of the device. For example, most of mechanical stimulation studies mainly focused on the topographical feature. In conventional electric-field stimulation studies, the electrodes were exposed to the cell culture medium. The long-term exposure of electrodes in the conducting cell culture medium typically results in a nonreversible Faradaic reaction, electrode degradation, and the production of harmful byproducts [17]. Cantilever-based studies mainly focused on the 3D organization of cardiomyocytes to elucidate the physiology of the cardiomyocytes [18], which is insufficient for improving tissue engineering *in vitro*. Therefore, a facile and efficient biosensing platform is required for improved tissue engineering and quantification of changes in the contractility behaviors of drug-treated cardiomyocytes.

With this research background and considering the advantages of both mechanical and electrical stimulation, herein, we propose a new cantilever platform to overcome the technical limitations of currently available cardiac toxicity screening methods. To the best of our knowledge, there are no reports on a cantilever-based device that simultaneously applies both mechanical and electrical stimulation. The surface-patterned SU-8 cantilever regulates cultured cardiomyocyte growth, morphology, and cell adhesion. The integrated electrical stimulator synchronizes the cardiomyocytes growing on the cantilever, thereby facilitating their maturation. The cardiomyocytes cultured on the SU-8 cantilever exhibited significantly improved maturation owing to the simultaneous mechanical and electrical stimulation. Fluorescence microscopy analysis and a western-blotting experiment were performed to demonstrate the enhanced cell maturation of the cultured cardiomyocytes. Furthermore, the proposed SU-8 cantilever platform was used to evaluate the adverse effects of different cardiovascular drugs, *i.e.*, verapamil, lidocaine, and isoproterenol, on the cardiomyocytes. In most of the previously reported studies, drug-treated cardiomyocytes often exhibited irregular beating behavior and an inconsistent beating cycle. In this study, these limitations were successfully overcome. The proposed SU-8 cantilever integrated with electrical and mechanical stimuli provided informative readouts, such as changes in the relative contraction force, rise time, and decay time of the drug-treated cardiomyocytes, which are beneficial for *in vitro* preclinical drug-screening applications.

2. Materials and methods

2.1. Device concept and fabrication of SU-8 cantilever-based stimulator

Fig. 1(a) shows the device concept of the proposed SU-8 cantilever-based cell culture platform. Fig. 1(b) shows a schematic view of the μgrooved electrode-integrated SU-8 cantilever and its operational principle. The device consists of a surface-patterned Au-electrode-integrated SU-8 cantilever, ~3-μm-pitch groove patterns, and a 0.5-μm laser reflecting electrode. The length (l), width (w), and thickness (d) of the cantilever are ~6 mm, 2 mm, and 16 μm, respectively. The calculated spring constant of the SU-8 cantilever is ~0.018 N/m. The length (l), width (w), and thickness (d) of the cantilever body are ~7 mm, 11 mm, and ~120 μm, respectively. The μgroove and electrical stimulator provide mechanical and electrical stimulation to the cultured cardiomyocytes. The integrated electrodes provide not only electrical stimulation but also impart compressive stress on the SU-8 cantilever during its operation, thereby simultaneously applying mechanical stimulation to the cultured cardiomyocytes.

Fig. 2 shows a detailed schematic illustration of the fabrication process flow for the μgrooved Au-electrode-integrated SU-8 cantilever. In a typical fabrication process, a 4-inch Si wafer was used as a substrate. Subsequently, a ~300-nm-thick silicon dioxide sacrificial thin film was grown on the Si substrate by a wet oxidation method. Then, a ~16-μm-thick SU-8 3010 (MicroChem, USA) photoresist was spin-coated on the sacrificial layer to form the cantilever structure. Thereafter, 10 nm/100 nm thick Ti/Au electrodes were deposited using an electron-beam deposition method. Next, ~3-μm-pitch groove patterns were defined on the cantilever surface using a thin SU-8 2002 (MicroChem, USA) photoresist. Finally, the cantilever body structure was formed using an SU-8 2050 (Microchem, USA) thick photoresist.

Fig. 3(a) shows an optical image of the μgrooved Au-electrode-integrated SU-8 cantilever before release from the Si substrate. The SiO_2 sacrificial layer was dissolved in a buffered oxide etchant and subsequently released the SU-8 cantilever from the Si substrate. Furthermore, additional cleaning processes such as flood exposure at 6000 mJ/cm^2, hard baking at 95 °C for 4 h, and sterilization in an autoclave were performed to improve the device stability and eliminate the toxicity of the fabricated devices. Fig. 3(b) shows an optical image of the Au-electrode-integrated SU-8 cantilever with electrical wires. A thin polydimethylsiloxane layer was coated on the wire bonding area to prevent the undesired electrical contact between the metal electrodes and the cell culture medium. Fig. 3(c) shows an optical image of the fabricated cantilever platform in a cell culture medium. A detailed description of experimental methods for neonatal rat ventricular myocyte (NRVM) isolation is provided in the online data supplement.

2.2. Electrical stimulation and measurement system

The cardiomyocytes were seeded on the Au-electrode-integrated SU-8 cantilever with surface patterns. Then, the cardiomyocytes were precultured for 72 h in a culture medium. Subsequently, electrical stimulation was performed by applying square monophasic pulses to the cardiomyocytes growing on the cantilevers. Before the drug-screening experiments, the electrical-stimulation parameters, such as bias voltage, frequency, and pulse duration, were optimized. The optimized stimulation parameters were a pulse duration of ~2 ms, a frequency of 0.5 Hz, and an amplitude of 500 mV. The distance between the two Au electrodes was ~1000 μm. The contraction force of the cardiomyocytes under electrical stimulation was monitored by measuring the displacement of the SU-8 cantilever. The cantilever displacement resulting from the contraction force of the cardiomyocytes was monitored at the free end of the SU-8 cantilever using a laser vibrometer. The LabVIEW-assisted laser vibrometer could measure the displacement with high accuracy even at the nanoscale. Fig. S1 shows a schematic of the experimental setup. The measurement system consisted of a signal generator, homemade stage top incubator, microscope, and motorized XYZ stage.

2.3. Statistical analysis

The obtained data were expressed as the average of at least three independent experimental data. The error bars represented the mean ± standard deviation (s.d.), with $n = 3$; $^*p < 0.05$ and $^{**}p < 0.01$ indicated statistical significance. The p values were measured *via* a one-way analysis of variance followed by Tukey's honest significant difference test.

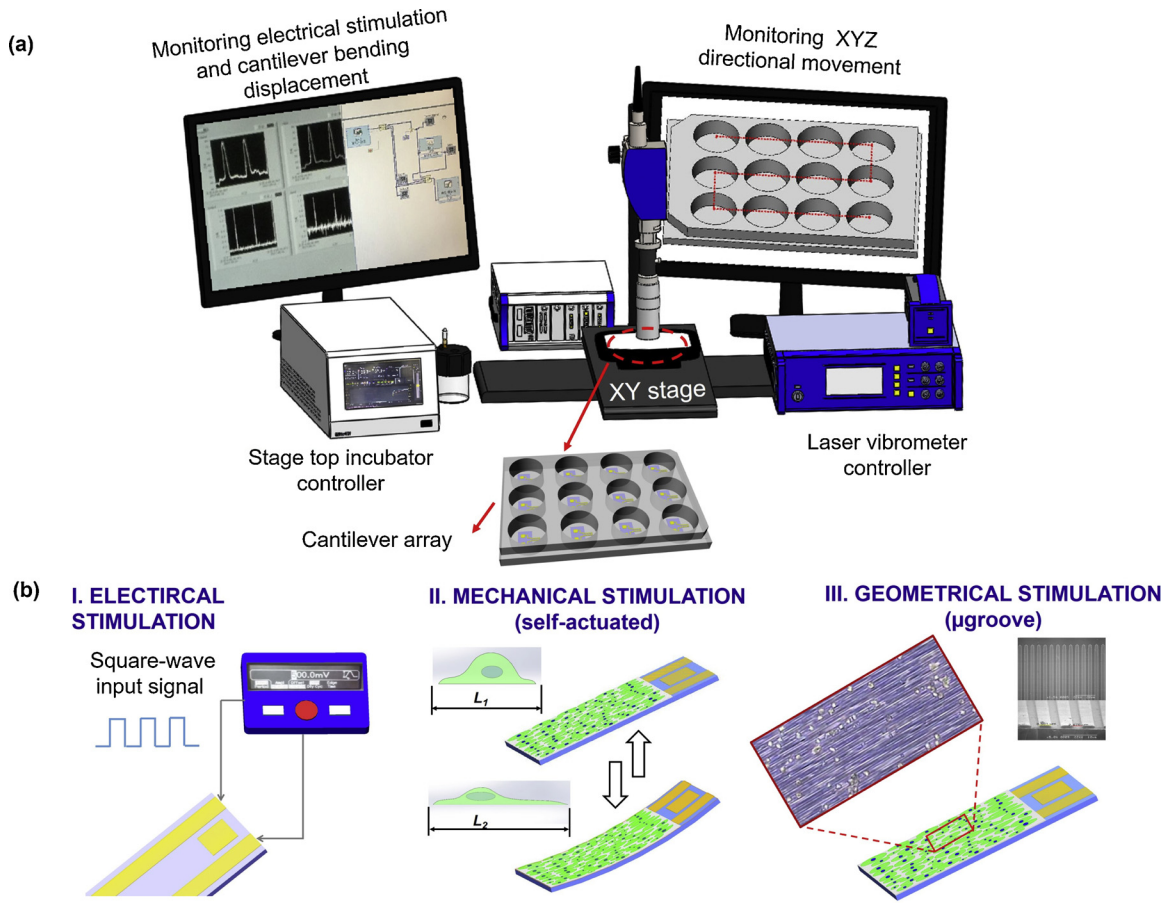

Fig. 1. (a) Schematic of a cell culture platform composed of the SU-8 cantilever integrated with electrical stimulation; **(b)** concept of multiple simulations using the cantilever device.

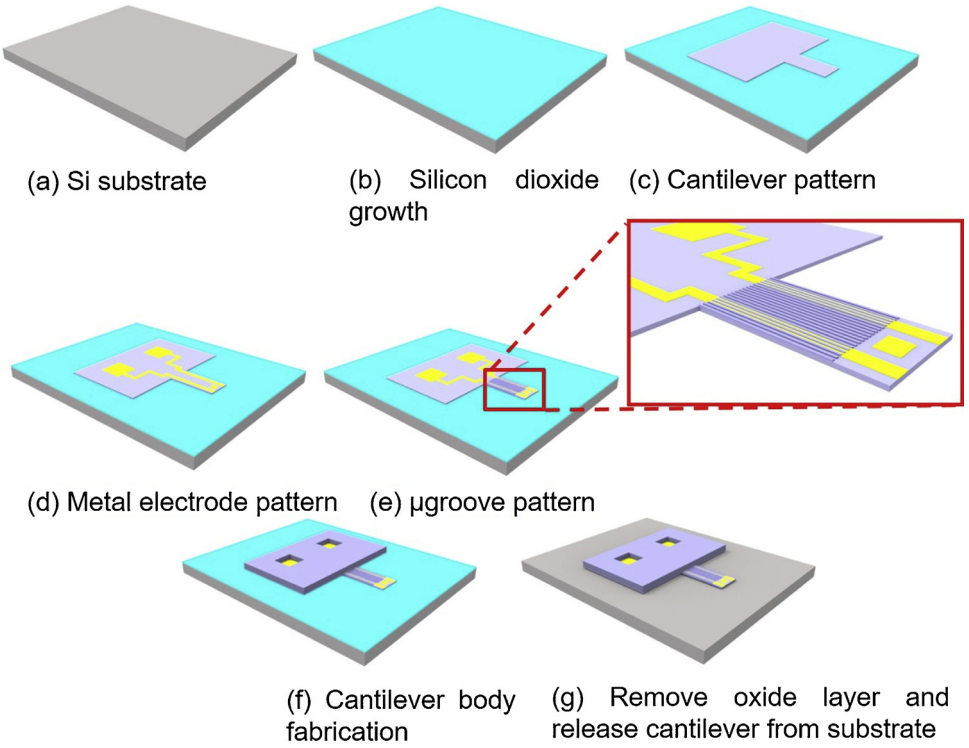

Fig. 2. Schematics of the fabrication process flow of the μgrooved Au-electrode-integrated SU-8 cantilever cell culture platform.

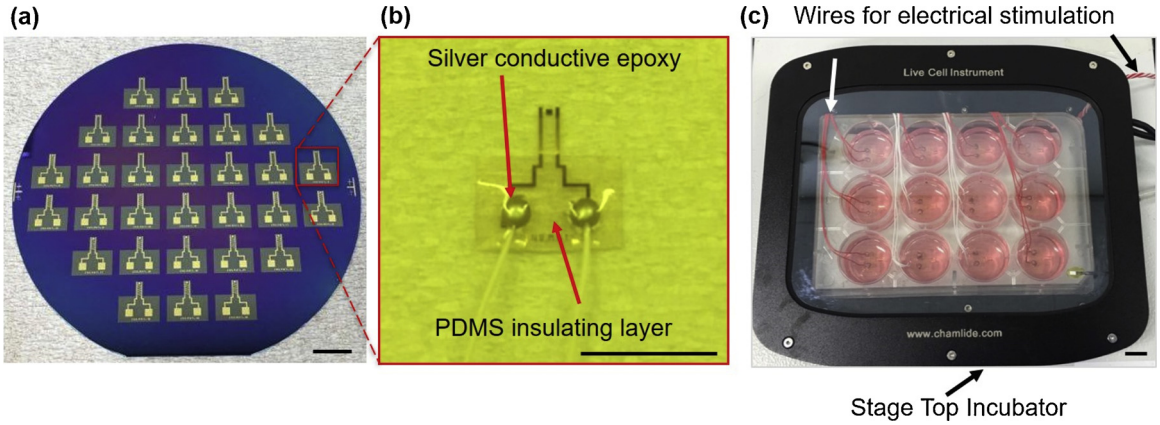

Fig. 3. Optical images of fabricated SU-8 cantilever device. **(a)** Top view of the cantilever structure before release from the Si wafer; **(b)** top view of fabricated cantilever with electrical wires; **(c)** top view of the cantilever array in the culture medium. The scale bar represents 10 mm.

3. Results and discussion

3.1. Material properties

Several SU-8-based biosensing platforms with excellent chemical stability and cell adhesion have been proposed [19]. First, the effects of the Young's modulus and surface energy of the SU-8 cantilever was investigated [20]. Second, the reliability of the Au electrode pattern formed on the SU-8 polymer was evaluated using an optical microscope. Fig. S2 shows optical images of the Au electrode pattern formed on the SU-8 substrate. A uniform Au electrode pattern was formed, without any wrinkles on the SU-8 substrate. The hydrophobic surface of an SU-8 polymer can be rendered hydrophilic by plasma treatment or chemical modification [21]. The water contact angle of the SU-8 polymer was examined before and after O_2 plasma treatment to determine the surface energy of the SU-8 polymer (Fig. S3). The water contact angles of the SU-8 polymer before and after O_2 plasma treatment were 90° and 14°, respectively. The water contact angle analysis indicates that the SU-8 surface is convenient for cell seeding. In addition, fibronectin protein was utilized as an extracellular matrix (ECM) which improves the adhesion between the cells and the substrate [22].

A soft substrate like a PDMS was also investigated as the candidate for cantilever materials. However, the PDMS was not very suitable for long-term cell culture due to the poor adhesion of the cells. Figure S4 shows the different morphologies of cardiomyocytes growing on different substrates. The cardiomyocyte adhesion was getting worse on the PDMS surface with increasing of the culture day (Fig. S4(a)). In contrast, cardiomyocyte proliferation and regeneration rates cultured on the SU-8 surface were more stable in comparing with the PDMS surface (Fig. S4(b)). The cardiomyocyte numbers with the covering area are shown in Fig. S4 c and d, respectively. These results indicate that the optimized substrate material significantly supports the strong adhesion of cardiomycoytes. Additionally, the cardiomyocytes cultured on the SU-8 surface without and with the O_2 plasma treatment exhibited excellent cell adhesion and maturation (Fig. S5(a–b)).

3.2. Optimization of μgroove patterns

It is well established that the μgroove patterns on the substrate strongly influence the elongation and maturation of cultured cardiomyocytes [23]. Therefore, the effect of groove patterns was optimized by measuring the contraction force of the cardiomyocytes cultured on the SU-8 cantilever patterned with different grooves. Groove patterns having 3–10 μm of width and 1 μm of depth were formed on the SU-8 substrates. Fig. S6(a) shows optical images of the various groove patterns formed on the SU-8 substrates. The acquired cardiomyocytes were seeded on the different grooved surfaces, and the α-sarcomere actinin length was measured on day 7 of the culturing period. The cardiomyocytes cultured on the SU-8 substrate with 3-μm grooves exhibited a significantly enhanced α-sarcomere actinin length (~1.7 μm) compared with that of the other μgroove substrates (Fig. S6(b)). Hence, we used 3 μm wide and 1 μm deep cantilever groove patterns for subsequent analysis. The obtained data indicate that the SU-8 was a suitable material for optimizing the cell shape, alignment, and adaptation of the cultured cardiomyocytes. The enhanced α-sarcomere actinin length observed on the SU-8 substrate was due to the appropriate SU-8 material stiffness, which was higher than nature cardiac elasticity behavior. The stiffness of the substrate can regulate cell growth, viability, and resistance to apoptosis [24]. Furthermore, the Young's modulus of the SU-8 material was ~2.2 GPa, which not only influenced the function of the myofibrils but also increased the cell adhesion and size of focal adhesion [25].

3.3. Contraction force measurement of cardiomyocytes

The displacement of the Au-electrode-integrated SU-8 cantilever resulting from the contraction force of the cardiomyocytes was monitored with respect to the cell culture period. The obtained cardiomyocytes were seeded on both micro-patterned and flat-surfaced SU-8 cantilevers with density of 1000 cell/mm^2. Figs. S7(a) and (b) show the displacement of the SU-8 cantilever as a function of the cell culture period. The contraction force of the cardiomyocytes gradually increased with increasing cell culture period. The cantilever exhibited the maximum displacement on day 10, which slightly decreased for both the flat-surfaced and μgrooved SU-8 cantilevers. The reduction in the cantilever displacement was due to the primary cell senescence and apoptosis in the *in vitro* environment without an electrical stimulus [11]. The bending displacement of two different cantilevers was characterized on day 10 after cell seeding. Herewith, the cantilever bending displacement caused by contraction and relaxation of the cardiomyocytes show the dynamic stretching phenomenon which is promoting intracellular organization, and extracellular tension. The maximum bending displacements were approximately 7.95 ± 0.2 μm for the flat-surfaced cantilever, and the values increased to 25.52 ± 0.3 μm for the μgrooved cantilever. The contraction forces of the cardiomyocytes on flat-surfaced and grooved cantilevers on day 10 were calculated using the spring constant of the fabricated cantilevers (0.018 N/m). The contraction force of the cardiomyocytes on day 10 was 0.143 ± 0.0036 μN for the flat-surfaced cantilever and 0.459 ± 0.0054 μN for the μgrooved cantilever. Higher bending displacement of the cantilever shows mechanical stretch for the cultured cardiomycytes. Continuous dynamic stretch help to promote maturation and contraction *via* hypertrophic pathway [22]. Figs. S7(c) and (d) show optical images of the cardiomyocytes cultured on the flat-surfaced and μgrooved SU-8

cantilevers, respectively on day 7 of the cell culture period. The length of the typical primary cardiac ventricular cells on the μgrooved SU-8 cantilever integrated with Au electrodes was ~100 μm.

3.4. Optimization of electrical stimulation parameters

The electrical-stimulation parameters were optimized using the 3-μm-grooved SU-8 cantilever (Fig. S8(a–b)). The cantilever displacement was monitored at different frequencies ranging from 0.2 to 2 Hz and pulse durations ranging from 0.5 to 50 ms. The cantilever displacement decreased with the increasing stimulation frequency. The displacement characteristics of the cantilever were completely changed when the frequency was increased above 1 Hz. At higher frequencies, the cantilever was unable to retain its original position, owing to the narrow frequency range of the applied electrical signal. The obtained results with respect to the applied frequency are presented in Fig. S9(a). The cantilever displacement and the beating duration of the cardiomyocytes obtained for 0.5 and 1 Hz exhibited small differences. The cantilever bending duration was more reasonable at 0.5 Hz than at 1 Hz. Additionally, the cantilever displacement was monitored under different square pulses with durations ranging from 0.5 to 50 ms (Fig. S9(b)). Tandon et al. reported that 2 ms is the optimal pulse duration for effective cantilever displacement [14]. In general, the optimal electrical field depends on the electrode materials. Charge injection of the Au electrode is higher than that of other electrode materials, and it does not cause a chemical reaction in the cell culture medium. According to the foregoing analysis, we conclude that 0.5 Hz applied frequency, 2 ms pulse duration, and 500 mV bias voltage were the optimal stimulation parameters for achieving the highest cantilever displacement. To elucidate the effect of electrical stimulation on the cardiomyocyte maturation, the electrical stimulation was applied for a long-term (7-d) period, as more mature cardiomyocytes may better reflect the physiology of the adult heart [26]. Therefore, investigation of the effect of the electrical stimulation on cultured cardiomyocytes is imperative for disease modeling and drug-screening applications. Fig. 4 shows the contraction force of the cardiomyocytes cultured on the SU-8 cantilever. The cardiomyocytes exhibited a significant difference in the contraction force depending on the culturing period, μgroove pattern, and electrical stimulation. The contraction force of the cultured cardiomyocytes increased with the cell culture period. The cardiomyocytes cultured on the μgrooved SU-8 cantilever with electrical stimulation exhibited a higher contraction force than those cultured on the flat-surfaced cantilever and the μgrooved SU-8 cantilever without electrical stimulation. The enhanced contraction force of the cardiomyocytes on the μgrooved Au-electrode-integrated SU-8 cantilever is attributed to the simultaneous mechanical and electrical stimulation.

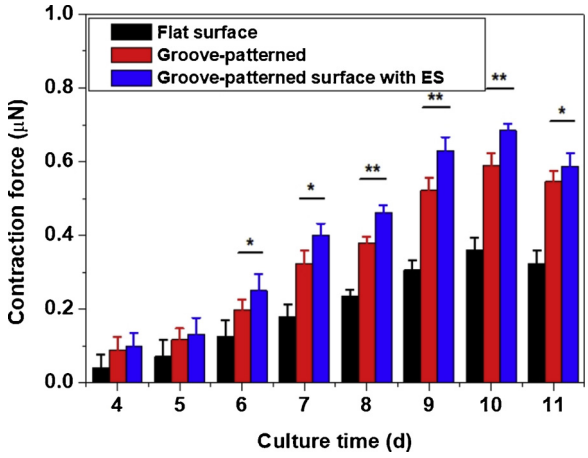

Fig. 4. Effect of long-term electrical stimulation on the contraction force of the cardiomyocytes. The contraction force of the cardiomyocytes cultured on the flat-surfaced and μgrooved SU-8 cantilevers with and without electrical stimulation. The error bars represent the mean ± s.d., with n = 3; *p < 0.05, **p < 0.01. "ES" represents "electrical stimulation.".

3.5. Immunocytochemistry (ICC) staining and western-blotting analyses

An ICC experiment was performed to confirm the expression of cardiomyocyte-growth regulating proteins, such as the myofibril structure-related protein α–actinin, the intracellular calcium-related protein TnT, and the transmembrane protein Connexin (Cx43). Fig. 5(a) and (b) show the α-sarcomere actinin length of the cardiomyocytes cultured without and with electrical stimulation, respectively. The both protocol of the ICC and western blotting was described in the online data supplement. Under electrical stimulation, the myofibrils were far more polarized, and the sarcomere length (green) of the cultured cardiomyocytes was significantly increased. The sarcomere length is an important indicator of contractile protein expression as it corresponds to the crosslinking of thin and thick filaments through this protein [24]. Fig. 5(c) shows the sarcomere length of the cardiomyocytes cultured with and without electrical stimulation. Owing to the electrical stimulation, the primary cardiac cell morphology was changed resulting in cardiomyocye maturation. The functionally mature primary cardiac cell has many advantages for *in vitro* tissue engineering assays. Additionally, the TnT protein is a marker protein expressed at intercellular sites as a cardiac-specific ultrastructural feature. As shown in Fig. 5(d), without electrical stimulation, cell growth was inferior, and cells showed less communication with neighboring cardiac cells. In contrast, with electrical stimulation (Fig. 5(e)), strong intracellular TnT (green color) expression was observed. Additionally, the expression of Cx-43 protein (red dots) in the cardiomyocytes increased under electrical stimulation compared with that without electrical stimulation. A high Cx-43 expression within the engineered cardiac tissue indicated electrical coupling, which is essential for proper anisotropic function. This suggests that the electrical stimulation enhanced the coupling and communication between the cells and resulted in higher cantilever displacements. Furthermore, protein markers, such as Cx-43, α-sarcomere actinin, and TnT, were quantitatively examined by western blotting. Their expression was significantly increased using the μgrooved SU-8 cantilever and simultaneous electromechanical stimulation (Fig. 5(f)). A control experiment was performed with a commercial well plate material, *i.e.*, polystyrene.

3.6. Drug-screening application

Finally, the applicability of the fabricated cantilever device for cardiovascular drug-screening applications was evaluated using cardiomyocytes treated with different cardiovascular drugs. The effects of the cardiac drugs on the cultured cardiomyocytes were assessed by monitoring the contraction force of the cardiomyocytes under simultaneous electrical and mechanical stimulations. Prior to the experiment, the cardiac drug diluting solution (ethanol) was evaluated to elucidate the influence of the solution on the cells. Fig.S10 shows the cantilever displacement for different concentrations of ethanol-treated cardiomyocytes. The cantilever displacement significantly decreased when the ethanol concentration reached ~1.5 % (v/v) and above. According to the experimental results and analysis, the ethanol concentration was fixed close to 0.1 % (v/v) to minimize the adverse effects of ethanol.

Several cardiovascular drug doses (Table S1) were selected according to the inhibitory concentration (IC_{50}) values from the Food and Drug Administration. Different concentrations of cardiovascular drugs were applied to the cardiomyocytes on day 8 of the culturing, as the cantilever displacement gradually increased on this day. Subsequently, the contraction force of the drug-treated cardiomyocytes was monitored by measuring the cantilever displacement. The cardiomyocytes seeded on the cantilever surface often produced an irregular beating behavior

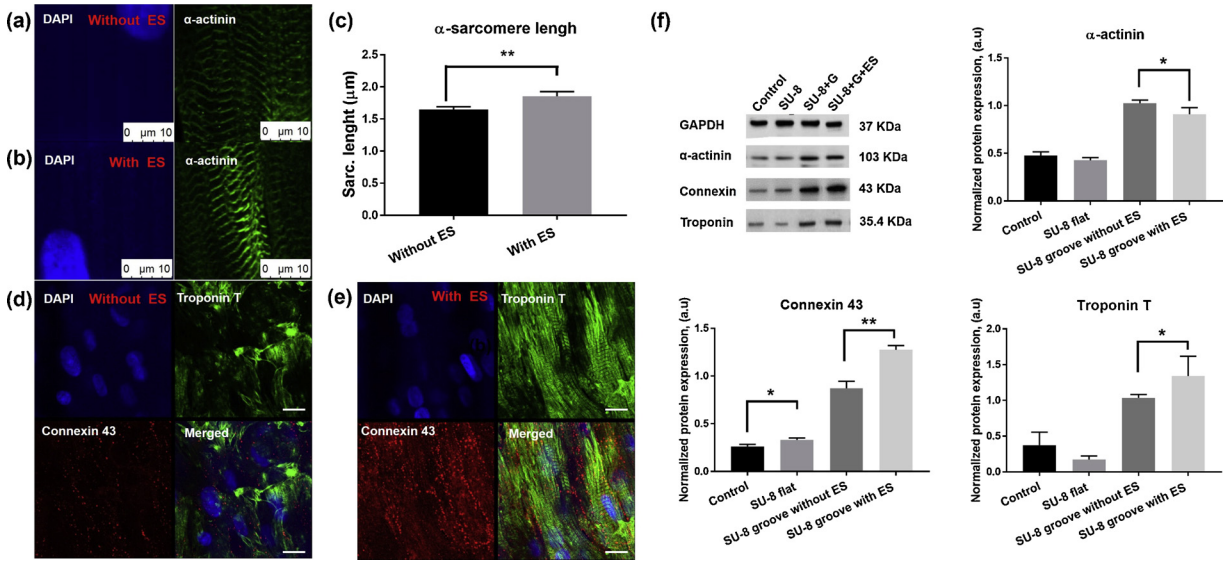

Fig. 5. Effect of long-term electrical stimulation on cardiac cell maturation. α-sarcomere actinin length of the cultured cardiomyocytes **(a)** without and **(b)** with electrical stimulation. **(c)** Bar plot presenting the α-sarcomere actinin length of the cultured cardiomyocytes without and with electrical stimulation. TnT and connexin 43 (Cx-43) protein expression of the cultured cardiomyocytes **(d)** without and **(e)** with electrical stimulation. **(f)** Western-blotting data showing the relative densities of major proteins—α-actinin, Cx-43, TnT, and GAPDH—expressed on different substrates. The error bars represent the mean ± s.d., n = 3; *p < 0.05, **p < 0.01. The scale bar represents 10 μm.

and an inconsistent beating cycle. The most beneficial achievement of the proposed Au-electrode-integrated cantilever is the easy control of the beating frequency of the cardiomyocytes during the drug test. Controlling the beating cycle of cardiomyocytes through electrical stimulation could improve the marginal effect of the cells.

Verapamil is a typical L-type Ca^{2+} channel blocker that inhibits the influence of Ca on cardiomyocytes [27]. The effect of verapamil on the cultured cardiomyocytes was evaluated by treating the cardiomyocytes with different concentrations of Verapamil (50, 150, 500, and 1000 nM). Fig. 6(a) and (b) show the relative contraction force of the cardiomyocytes treated with different concentrations of verapamil without electrical stimulation. The relative contraction force of the cardiomyocytes gradually decreased with the increasing verapamil concentration. The relative contraction force of the cardiomyocytes was reduced by ~40 % compared with the control state at a concentration of 500 nM. Additionally, the beating duration of the cardiomyocytes was reduced at higher verapamil concentrations. Fig. 6(c) and (d) show the rise and decay times of the cardiomyocytes at different verapamil concentrations. With the increasing verapamil concentration, the rise and decay times of the cardiomyocytes increased and decreased, respectively.

Under electrical stimulation, the relative contraction force of the cardiomyocytes was reduced by ~50 % at 500 nM, but the beating frequency of the cardiomyocytes was maintained (Fig. 6(e) and (f)). However, at a high concentration of verapamil (1000 nM), the beating duration of the cardiomyocytes was unable to be controlled although the frequency was 0.5 Hz. This indicated that a high concentration of verapamil blocks Ca^{2+} channels and changes the behavior of the ion flow in the action potential. A precarious state in the ion flux causes an irregular beating duration, which cannot be controlled *via* electrical stimulation. Fig. 6(g) and (h) show the rise and decay times for the cardiomyocytes treated with different concentrations of verapamil

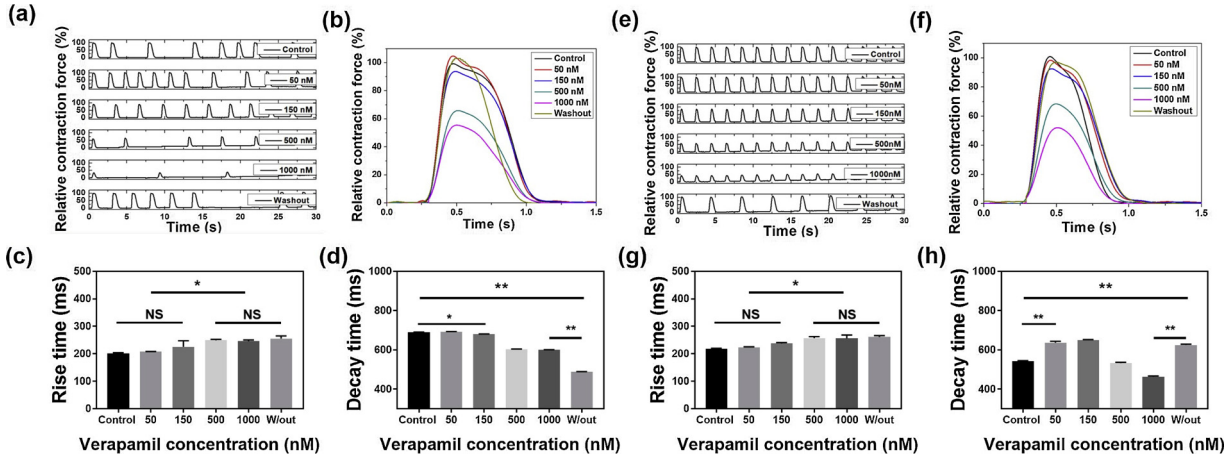

Fig. 6. Mechanical response for the cardiomyocytes treated with different concentrations of verapamil. **(a)** Relative contraction force of the cardiomyocytes without electrical stimulation. **(b)** Changes of the relative contraction force and the frequency for the cardiomyocytes treated with different concentrations of verapamil without electrical stimulation. **(c, d)** Rise and decay times of the cardiomyocytes treated with different concentrations of verapamil. **(e)** Relative contraction force of the cardiomyocytes with electrical stimulation. **(f)** Changes of the relative contraction force and frequency for the cardiomyocytes treated with different concentrations of verapamil with electrical stimulation. **(g, h)** Rise and decay times of the cardiomyocytes treated with different concentrations of verapamil with electrical stimulation. The error bars represent the mean ± s.d., with n = 3; *p < 0.05, **p < 0.01.

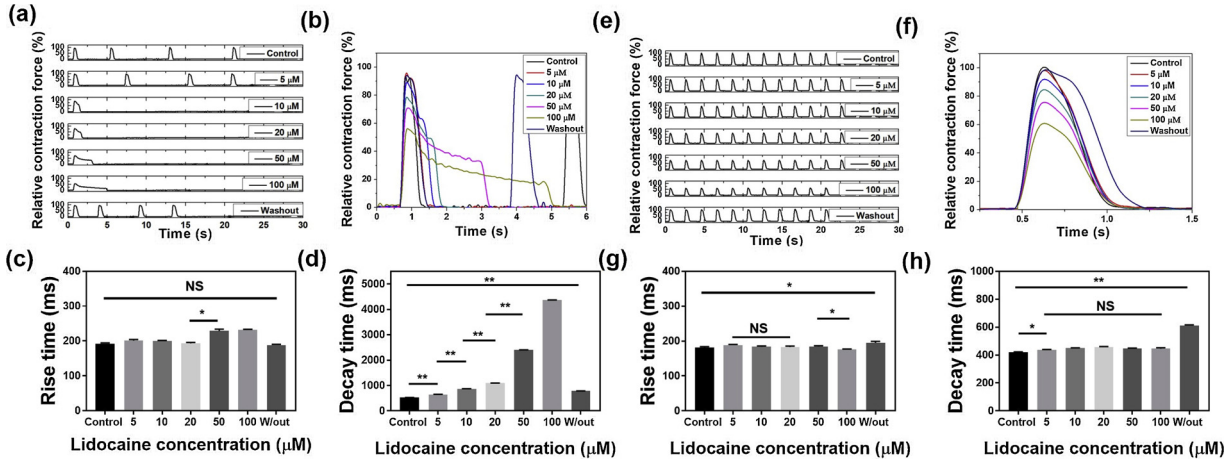

Fig. 7. Mechanical response for the cardiomyocytes treated with different concentrations of lidocaine. **(a)** Relative contraction force of the cardiomyocytes without electrical stimulation. **(b)** Changes of the relative contraction force and frequency for the cardiomyocytes treated with different concentrations of lidocaine without electrical stimulation. **(c, d)** Rise and decay times of the cardiomyocytes treated with different concentrations of lidocaine. **(e)** Relative contraction force of the cardiomyocytes with electrical stimulation. **(f)** Changes of the relative contraction force and frequency for the cardiomyocytes treated with different concentrations of lidocaine with electrical stimulation. **(g, h)** Rise and decay times of the cardiomyocytes treated with different concentrations of lidocaine with electrical stimulation. The error bars represent the mean ± s.d., with n = 3; *p < 0.05, **p < 0.01.

under electrical stimulation. With the increasing verapamil concentration, the rise time of the cardiomyocytes increased, whereas the decay time of the cardiomyocytes increased to 150 nM and then decreased. Finally, the drug-treated cardiomyocytes were washed three times with a cardiomyocyte plating medium and allowed to equilibrate for 20 min in an incubator, and all the parameters were measured again. The relative contraction force of the cardiomyocytes was close to the control state. Although the relative contraction force returned to its initial value, the damaged cardiomyocytes were not synchronized by electrical stimulation, indicating that a high concentration of verapamil induced a severe side effect on the cardiomyocytes.

Lidocaine, which is known as a Na channel blocker, has been used to determine the relationship between cardiac contractility and toxicity changing the drug concentration. Generally, lidocaine causes low blood pressure and an irregular heart rate; therefore, it is crucial to study its effect on the cardiomyocytes. When the lidocaine concentration increased above the threshold value (20 μM), it affected the cell beating frequency [28]. Different concentrations of lidocaine (5–100 μM) were applied to the cultured cardiomyocytes, and the contractility behavior was measured with and without electrical stimulation. Fig. 7(a) and (b) show the relative contraction force of the cardiomyocytes treated with different concentrations of lidocaine without electrical stimulation. The relative contraction force of the cardiomyocytes decreased with the increasing drug concentration. However, the beating duration of the cardiomyocytes increased with the lidocaine concentration. After the drug-treated cardiomyocytes were washed with a plating medium, the relative contraction force and cell beating frequency returned to their initial values. Fig. 7(c) and (d) show the rise and decay times of the cardiomyocytes at different Lidocaine concentrations. The result shown that the rise time was not significant difference while decay time increased significantly at higher lidocaine concentrations.

In contrast, in the presence of electrical stimulation (Fig. 7(e) and (f)), the cell beating frequency and beating duration were fixed within certain ranges. In the case of a single beating cycle, the relative contraction force gradually decreased with the increasing lidocaine concentration. The electrical stimulation significantly affected the rise and decay times of the cardiomyocytes treated with different concentrations of lidocaine (Fig. 7(g) and (h)). The obtained results indicate that the lidocaine strongly influenced the contraction force of the cardiomyocytes, rather than the beating frequency. Therefore, lidocaine has an insignificant side effect on cardiomyocytes even after the drug is washed with a plating medium [29].

Isoproterenol is a β-1 agonist of the adrenergic receptor and produces a positive cardiac inotropic effect [12]. The cultured cardiomyocytes were treated with different concentrations of isoproterenol, and the contractile behavior was evaluated with and without electrical stimulation. Fig. 8(a) and (b) show the relative contraction force and beating frequency of the cardiomyocytes treated with different concentrations of isoproterenol. The relative contraction force of the cardiomyocytes consistently increased as the isoproterenol concentration increased to 1 μM and then decreased with a further increase in the drug concentration. The beating duration of the cardiomyocytes decreased with an increase in the isoproterenol concentration above 1 μM. The relative contraction force of the cardiomyocytes increased by ~10 % as the isoproterenol concentration increased to 1 μM and then decreased. With the increasing isoproterenol concentration, the beating pattern of the cardiomyocytes became irregular, and a tachycardia sequence was observed. Fig. 8(c) and (d) show the rise and decay times of the cardiomyocytes treated with different concentrations of isoproterenol.

Fig. 8(e) and (f) show the relative contraction force of the cardiomyocytes treated with different concentrations of isoproterenol under electrical stimulation. The irregular beating pattern of the cardiomyocytes significantly decreased with the increasing isoproterenol concentration and was affected by the electrical stimulation. The rise and decay times of the cardiomyocytes treated with different concentrations of isoproterenol are shown in Fig. 8(g) and (h). As discussed in the previous section, the SU-8 cantilever with mechanical/electrical stimulation facilitated the maturation of the cardiomyocytes, improving their physiological phenotypes. The μgrooved SU-8 cantilever integrated with Au electrodes provided new information regarding drug toxicity. As shown in Figs. 6–8, the contractile behavior revealed the effects of different cardiovascular drugs on the cultured cardiomyocytes.

Finally, the SU-8 cantilevers were employed for the preliminary study of induced pluripotent stem cell-derived cardiomyocytes (hiPSC-CMs) in toxicity screening. Fig. S11(a) shows the preparation process of the hiPSC-CMs. The uniform distribution of the hiPSC-CMs on the surface of the SU-8 cantilever was confirmed using the images of the optical microscope. Fig. S11(b) shows the SU-8 cantilever displacement on the 7th day of the culture period. The contraction force of the hiPSC-CMs cultured on the cantilever with and without microgroove pattern is shown in Fig. S12. The hiPSC-CMs cultured on the microgroove patterned SU-8 cantilever exhibits the higher contraction force compared

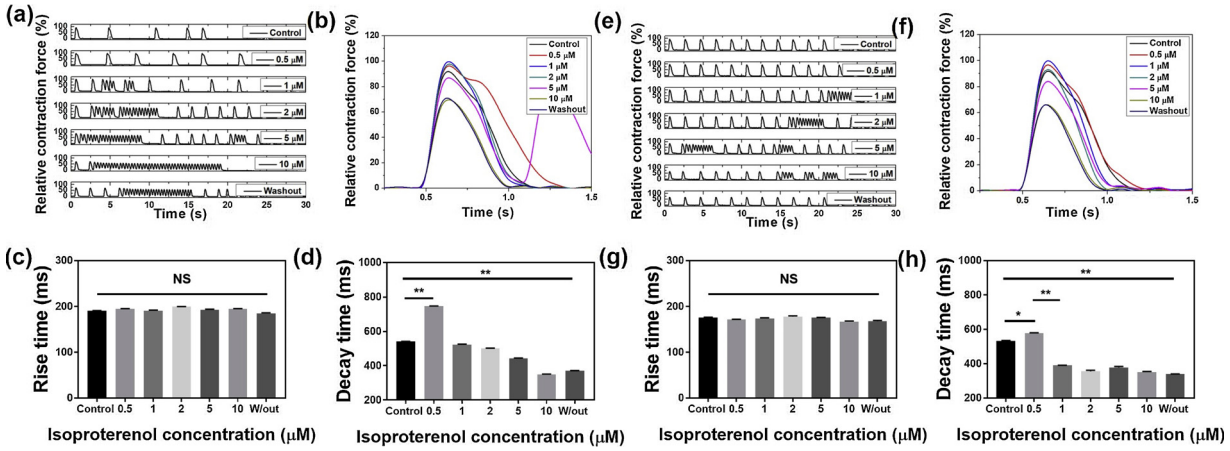

Fig. 8. Mechanical response for the cardiomyocytes treated with different concentrations of isoproterenol. **(a)** Relative contraction force of the cardiomyocytes without electrical stimulation. **(b)** Changes of the relative contraction force and frequency for the cardiomyocytes treated with different concentrations of isoproterenol without electrical stimulation. **(c, d)** Rise and decay times of the cardiomyocytes treated with different concentrations of isoproterenol. **(e)** Relative contraction force of the cardiomyocytes with electrical stimulation. **(f)** Changes of the relative contraction force and frequency for the cardiomyocytes treated with different concentrations of isoproterenol with electrical stimulation. **(g, h)** Rise and decay times of the cardiomyocytes treated with different concentrations of isoproterenol. The error bars represent the mean ± s.d., with n = 3; *p < 0.05, **p < 0.01.

to that flat surface SU-8 cantilever. The contraction force of the hiPSC-CMs increased with the culture period and reached the highest contraction force on day 7. The preliminary sensor characteristics indicate that the proposed cantilever system could be used for the toxicity analysis based on the hiPSC-CMs. Furthermore, the proposed SU-8 cantilever arrays can be used as a high throughput drug screening platform by scaling up the fabricated 12 well plate assay into 192 cantilever arrays. To scale up the current sensor system, we also designed a motorized stage based high throughput drug screening system that can measure 192 cantilever arrays in real-time. We anticipate that the proposed sensors array provides an opportunity to develop the next generation of biomedical devices for cardiotoxicity testing using human cells.

4. Conclusion

An SU-8 cantilever-based electrophysiological stimulating platform was developed and characterized. The proposed cantilever platform with μgrooved patterns effectively aligned cardiomyocytes on the cantilever. The use of the unique cantilever design increased the contraction force of cardiomyocytes up to three times that of conventional cantilevers. Additionally, electromechanical stimulation promoted the maturation of the cardiomyocytes during the culturing period. According to the experimental results, the proposed SU-8 cantilever platform accompanied by electromechanical stimulation is excellent for accurately determining the effects of different cardiovascular drugs on the cardiomyocyte contraction force and beating durations.

Declaration of Competing Interest

The authors declare no conflicts of interest.

Acknowledgements

This study was supported by a National Research Foundation of Korea grant funded by the Ministry of Science and ICT (2017R1E1A1A01074550) and the Korea Health Technology R&D Project funded by the Ministry of Health & Welfare (HI19C0642), Republic of Korea.

Appendix A. Supplementary data

Supplementary material related to this article can be found, in the online version, at doi:https://doi.org/10.1016/j.colsurfb.2019.110682.

References

[1] H. Iso, EPMA J. 2 (2011) 49.
[2] E.J. Benjamin, M.J. Blaha, S.E. Chiuve, M. Cushman, S.R. Das, R. Deo, S.D. de Ferranti, J. Floyd, M. Fornage, C. Gillespie, C.R. Isasi, M.C. Jimenez, L.C. Jordan, S.E. Judd, D. Lackland, J.H. Lichtman, L. Lisabeth, S. Liu, C.T. Longenecker, R.H. Mackey, K. Matsushita, D. Mozaffarian, M.E. Mussolino, K. Nasir, R.W. Neumar, L. Palaniappan, D.K. Pandey, R.R. Thiagarajan, M.J. Reeves, M. Ritchey, C.J. Rodriguez, G.A. Roth, W.D. Rosamong, C. Sasson, A. Towfighi, C.W. Tsao, M.B. Turner, S.S. Virani, J.H. Voeks, J.Z. Willey, J.T. Wilkins, J.H.Y. Wu, H.M. Alger, S.S. Wong, P. Muntner, Circulation (2017).
[3] J. Feenstra, D.E. Grobbee, W.J. Remme, B.H.C. Stricker, JACC 33 (1999) 1152.
[4] T. Danker, C. Moller, Front. Pharmacol. 5 (2014) 203.
[5] A. Pointon, A.R. Harmer, I.L. Dale, N. Abi-Gerges, J. Bowes, C. Pollard, H. Garside, Toxicol. Sci. 144 (2015) 227.
[6] M. Maddah, J.D. Heidmann, M.A. Mandegar, C.D. Walker, S. Bolouki, B.R. Conklin, K.E. Loewke, Stem Cell Rep. 4 (2015) 624.
[7] B.M. Maoz, A. Herland, O.Y.F. Henry, W.D. Leineweber, M. Yadid, J. Doyle, R. Mannix, V.J. Kujala, E.A. Fitzgelard, K.K. Parker, D.E. Ingber, Lab Chip 17 (2017) 2294.
[8] A.F.G. Godier-Furnemont, M. Tiburcy, E. Wagner, M. Dewenter, S. Lammle, A. El-Armouch, S.E. Lehnart, G. Vunjak-Novakovic, W.H. Zimmermann, Biomaterials 60 (2015) 82.
[9] N.E. Oyunbaatar, D.H. Lee, S.J. Patil, E.S. Kim, D.W. Lee, Sensors 16 (2016) 1258.
[10] D. Carson, M. Hnilova, X. Yang, C.L. Nemeth, J.H. Tsui, A.S.T. Smith, A. Jiao, M. Regnier, C.E. Murry, C. Tamerler, D.H. Kim, ACS Appl. Mater. Interfaces 8 (2016) 21923.
[11] Y. Dai, N.-E. Oyunbaatar, B.K. Lee, E.S. Kim, D.W. Lee, Sens. Actuators B 255 (2018) 3391.
[12] J.Y. Kim, Y.S. Choi, B.K. Lee, D.W. Lee, Biosens. Bioelectron. 80 (2016) 456.
[13] L.M. Monteiro, F. Vasques-Novoa, L. Ferreira, P. Pinto-do-O, D.S. Nascimento, Restoring heart function and electrical integrity: closing the circuit, NPJ Regen. Med. 9 (2017) 1.
[14] N. Tandon, A. Marsano, R. Maidhof, K. Numata, C. Montouri-Sorrentino, C. Cannizzaro, J. Voldmand, G. Vunjak-Novakovic, Lab Chip 10 (2010) 692.
[15] W. Bian, L. Tung, Circ. Res. 28 (2006) e29.
[16] F. Qian, C. Huang, Y.D. Lin, A.N. Ivanovskaya, T.J. O'Hara, R.H. Booth, C.J. Creek, H.A. Enright, D.A. Soscia, A.M. Belle, R. Liao, F.C. Lightstone, K.S. Kulp, E.K. Wheeler, Lab Chip 17 (2017) 1732.
[17] N. Tandon, A. Marsano, R. Maidhof, L. Wan, H. Park, G. Vunjak-Novakovis, J. Tissue Eng. Regen. Med. 5 (2011) e115.
[18] A. Grosberg, P.W. Alford, M.L. McCain, K.K. Parker, Lab Chip 11 (2011) 4165.
[19] V. Martinex, P. Behr, U. Drechsler, J. Polesel-Martis, J. Potthoff, E. Voros, T. Zambelli, J. Micromech. Microeng. 26 (2016) 055006.
[20] J.G. Jacot, A.D. Mcculluch, J.H. Omens, Biophys. J. 95 (2008) 3479.
[21] M. Nordstrom, R. Marie, M. Calleja, A. Boison, J. Micromech. Microeng. 14 (2004) 1614.
[22] T.J. Herron, A.M. Da Rocha, K.F. Campbell, D. Ponce-Balbuena, B.C. Willis,

G. Guerrero-Serna, Q. Liu, M. Klos, H. Musa, M. Zarzoso, A. Bizy, J. Furness, J. Anumonwo, S. Mironov, J. Jalife, Circ. Arryhythm Electrophysiol. 9 (2016) e003638, , https://doi.org/10.1161/CIRCEP.113.003638.
[23] D.S. Kim, Y.J. Jeong, B.K. Lee, A. Shanmugasundaram, D.W. Lee, Sens. Actuators B Chem. 240 (2017) 566.
[24] A.G. Rodriguez, S.J. Han, M. Regnier, N.J. Sniadecki, Biophys. J. 101 (2011) 2455.
[25] R.G. Wells, Hepatology 47 (2008) 1394.
[26] Y.C. Chan, S. Ting, Y.K. Lee, K.M. Ng, J. Zhang, Z. Chen, C.W. Siu, S.K.W. Oh, H.F. Tse, J. Cardiovasc. Trans. Res. 6 (2013) 989.
[27] P. Liang, F. Lan, A.S. Lee, T. Gong, V. Sanchez-Freire, Y. Wang, S. Diecke, K. Sallam, J.W. Knowles, P.J. Wang, P.K. Nguyen, D.M. Bers, R.C. Robbins, J.C. Wu, Circulation 127 (2013) 1677V.
[28] V.A. Maltsev, H.N. Sabbah, M. Tanimura, M. Lesch, S. Goldstein, A.I. Undrovinas, CMLS, Cell. Mol. Life Sci. 54 (1998) 597.
[29] A. Sathaye, N. Bursac, S. Sheehy, L. Tung, J. Mol. Cell Cardiol. 41 (2006) 633.